The Meteoritical Society

Meteoritics & Planetary Science 56, Nr 3, 586–600 (2021)
doi: 10.1111/maps.13638

Amino acid abundances and compositions in iron and stony-iron meteorites

Jamie E. ELSILA[1]*, Natasha M. JOHNSON[1], Daniel P. GLAVIN[1], José C. APONTE[1,2], and Jason P. DWORKIN[1]

[1]NASA Goddard Space Flight Center, Greenbelt, Maryland 20771, USA
[2]Department of Physics, Catholic University of America, Washington, District of Columbia 20064, USA
*Corresponding author. E-mail: jamie.elsila@nasa.gov

(Received 06 October 2020; revision accepted 17 January 2021)

Abstract–The organic compositions of carbonaceous chondrite meteorites have been extensively studied; however, there have been fewer reports of other meteorite classes, and almost none from iron meteorites, which contain much less carbon than carbonaceous chondrites but make up ~4% of observed meteorite falls. Here, we report the bulk amino acid content of three iron meteorites (Campo del Cielo, IAB; Canyon Diablo, IAB; and Cape York, IIIAB) and both the metal and silicate portions of a pallasite (Imilac). We developed a novel method to prepare the samples for analysis, followed by hot water extraction and analysis via liquid chromatography-mass spectrometry. Free amino acid abundances ranging from 301 to 1216 pmol g^{-1} were observed in the meteorites, with the highest abundance in the silicate portion of the pallasite. Although some of the amino acid content could be attributed to terrestrial contamination, evidence suggests that some compounds are indigenous. A suite of C_5 amino acids was observed with a distinct distribution favoring a straight chain (*n*-pentanoic acid) structure; this straight chain dominance is suggestive of that observed in thermally altered stony meteorites. Amino acids were also observed in terrestrial iron granules that were milled and analyzed in the same way as the meteorites, although the distribution of detected amino acids was different. It is possible that similar formation mechanisms existed in both the meteorites and the terrestrial iron, or that observed amino acids resulted from reactions of precursors during sample preparation. This work suggests that iron meteorites should not be overlooked for contributions of amino acids and likely other soluble organic molecules to the early Earth. Future studies of iron–nickel meteorites and asteroids, such as Psyche, may provide further insights into their potential organic inventory.

INTRODUCTION

There have been many studies of the organic content of meteorites as a means of understanding both the chemistry of the early solar system and the potential delivery of organic materials to the early Earth. A wide variety of organic compounds have been identified in meteorites, including amino acids, amines, hydrocarbons, carboxylic acids, sugars, nucleobases, and many more (e.g., Sephton [2002]; Pizzarello et al. [2006]; Glavin et al. [2018] and references therein). Amino acids, which are the monomers of proteins and are essential to life on Earth, are one of the most heavily studied classes of organic compounds. Amino acids have been observed in varying abundances and distributions in representatives of many types of stony meteorites, including all eight carbonaceous chondrite groups (CO, CV, CK, CI, CM, CR, CB, and CH), as well as in ungrouped carbonaceous chondrites, ordinary and R chondrites, and achondrites (Elsila et al. [2016] and references therein).

Beyond carbonaceous chondrites and the other stony meteorites, however, iron meteorites or iron-stony pallasites are also potential repositories of organic compounds and could have delivered prebiotic material to the early Earth. Iron meteorites comprise ~4% of falls to the Earth (where a "fall" is a meteorite that was observed to fall from the sky), but make up ~48% by mass of recorded meteorite falls (Grossman 2018;

Korotev 2020). Iron meteorites are classified as belonging to one of 13 groups or as "ungrouped" (Chabot et al. [2006] and references therein). The groups themselves can be described as two main types (1) magmatic meteorites that appear to have formed by fractional crystallization in the molten cores of differentiated asteroids and (2) nonmagmatic meteorites, also described as primitive achondrites that often contain silicate inclusions of primitive chondritic composition. The magmatic meteorites can also be split into groups that appear to have derived from melted carbonaceous chondrite-like precursors and into noncarbonaceous groups (Kruijer et al. 2017). Pallasites are assemblages of olivine and metal that may be samples from the core–mantle boundary of asteroid-sized parent bodies (Chabot et al. [2006] and references therein). Iron meteorites are known to contain carbon, in the form of graphite, carbides, and dissolved in the Fe-Ni metal; the carbon is not distributed homogeneously, making it difficult to report meaningful bulk carbon composition (Buchwald 1975; Sugiura 1998; Grady and Wright 2003).

The metal surfaces or the interfaces between silicate and metal in meteorites are potential sites for chemical reactions, including amino acid synthesis. Analyses of carbonaceous chondrites provide some support for this hypothesis. The CR clan of carbonaceous chondrites comprises CR chondrites (~5 vol% metal) as well as the more metal-rich CH (~20 vol% metal) and CB (60–80 vol% metal) chondrites; all of these groups contain amino acids, with abundances of 70–124 nmol g^{-1} for unhydrolyzed hot water extracts from CH chondrites and 1.1–10.2 nmol g^{-1} for CB chondrites (Burton et al. 2013). The amino acid distributions of CH and CB chondrites differ from those seen in lower-metal aqueously altered CM and CR chondrites, with elevated levels of straight chain, terminal amine amino acids (*n*-ω-amino acids) compared to α-amino acids, which are more common in the CM and CR chondrites. This dominance of *n*-ω-amino acids has previously been hypothesized to be a signature of Fischer–Tropsch/Haber–Bosch-type surface-catalyzed reactions (Burton et al. 2012), which could occur from reactions of gases such as CO, H_2, and NH_3 on metal or mineral grains on a cooling parent body. The presence of this amino acid distribution in the metal-rich CH and CB chondrites suggests the possibility of amino acid formation in other metal-rich meteorites such as irons, in particular IAB iron meteorites with carbon-containing inclusions. This hypothesis is also strengthened by experiments showing that material from iron meteorites can catalyze the formation of amino acids from mixtures of carbon monoxide, ammonia, and hydrogen (Hayatsu et al. 1971; Yoshino et al. 1971; Pizzarello 2012). Recent studies suggest that impacts of iron meteorites into early Earth oceans could lead to the formation of amino acids from reactions of atmospheric CO_2 and N_2 (Takeuchi et al. 2020), while physical impacts of iron cyano complexes are also hypothesized to lead to amino acid precursors (Bolm et al. 2018). Aqueous corrosion of iron meteorites in Earth's oceans may also have released soluble compounds from these meteorites into the environment (Pasek and Lauretta 2005). Iron meteorites could therefore be significant in several potential amino acid synthesis pathways.

CB and CH chondrite analyses have also revealed enantiomeric excesses in isovaline (Burton et al. 2013), a five-carbon (C_5) amino acid that is uncommon in the terrestrial biosphere. Although abiotic chemistry should produce racemic mixtures of chiral compounds in the absence of a chiral driving force, enantiomeric excesses of certain amino acids, including isovaline, have been observed in a variety of meteorites. The L-isovaline excesses observed in CB (up to 14%) and CH (up to 20%) chondrites are among the highest reported (Burton et al. 2013; Glavin et al. 2020). Rosenberg et al. (2008) showed that spin-polarized secondary electrons emitted from the photolysis of an iron–nickel magnetic substrate result in chiral selective reactivity of (*R*)- or (*S*)-2-butanol. This suggests a possible mechanism where the proximity to iron–nickel in a meteorite parent body could induce chiral selection in amino acids, although this may be most relevant to those meteorites that record remanent magnetic fields. This raises the possibility that enantiomeric enrichment could be occurring due to, or at least correlated with, the presence of high volumes of metal and metal–silicate interfaces, leading to an interest in examining amino acid enantiomeric composition in iron meteorites. Although it has been suggested that a similar result might also occur from the production of spin-polarized electrons through β-decay of ^{60}Fe inside a parent body in the early solar system, the effect of the polarized electrons from energetic β-decay would be obscured by a cascade of low-energy, unpolarized secondary electrons (Rosenberg [2011] and references therein). Magnetochiral anisotropy has also been suggested as a source of enantiomeric excesses due to interactions between organic compounds and ferromagnetic materials (Rikken and Raupach 2000; Pizzarello and Groy 2011; Cooper et al. 2020).

To the best of our knowledge, there have been no previously reported studies of amino acids in iron meteorites or pallasites. This may be due to the difficulties in powdering iron meteorite samples that is required for efficient extraction analysis of soluble organic compounds from such samples, or due to their trace total carbon abundances and low expectations of organic compounds forming or surviving in their parent

body environments. Paraffinic hydrocarbons and isoprenoids were observed inside and outside graphite–troilite nodules from the Canyon Diablo and the Odessa IAB iron meteorites (Nooner and Oró 1967), but these were likely terrestrial contaminants. Although the soluble organic composition of iron meteorites has not previously been investigated in detail and they only represent a few percent of all meteorites that have been found on Earth, they account for nearly half of the total meteorite mass (Grossman 2018; Korotev 2020); therefore, iron meteorites could have been important contributors to the prebiotic organic inventory of the early Earth. Here, we report the first analyses of amino acids in iron meteorites, as well as in the metal and silicate portions of a pallasite and in control materials. We include analyses of two IAB meteorites, a group of nonmagmatic iron meteorites that typically contain silicate inclusions, as well as one IIIAB meteorite, a group of magmatic iron meteorites that does not have substantial silicate inclusions.

MATERIALS AND METHODS

Meteorite Samples

Table 1 lists the meteorite samples analyzed in this study. Iron meteorite and pallasite samples were provided by the Division of Meteorites, Department of Mineral Sciences, Smithsonian Institution; all analyses were on bulk materials with no analyses of silicate or graphite–troilite inclusions or subsections performed. Samples were cut at the Smithsonian using abrasive saw blades that are composed of a rubber-based bonding compound that holds the abrasive grains that do the cutting. The coolant is a flood of municipal tap water; specimens were dried after cutting by heating on a hot plate. No elemental or mineralogical characterization was performed on these samples.

Prior to meteorite processing and extraction at NASA Goddard Space Flight Center (GSFC), the iron meteorite fragments were sonicated individually in 2 mL of ultrapure water (18.2 MΩ, <3 ppb total organic carbon, Millipore Milli-Q Integral 10 system) for 30 min at room temperature to remove contamination from their exteriors. The wash water from the Campo del Cielo and Canyon Diablo meteorites was analyzed as a control for external contamination from cutting and handling.

Meteorite Processing and Extraction

All glassware, ceramics, and sample handling tools used in sample processing were rinsed with ultrapure water (18.2 MΩ, <3 ppb total organic carbon), wrapped in aluminum foil, and then heated in a furnace at 500 °C in air overnight.

Table 1. Meteorite samples analyzed in this study.

Meteorite (class)	Sample	Unhydrolyzed analysis mass (g)
Campo del Cielo (IAB)	USNM 5620 2	0.3380
Canyon Diablo (IAB)	USNM 1725	0.7739
Cape York (IIIAB)	USNM 5727 25	0.9845
Imilac pallasite metal	USNM 1333	0.6519
Imilac pallasite silicate	USNM 1333	0.4422

The cohesion and malleability of iron meteorites mean that our typical method used for preparing stony meteorites (i.e., grinding a sample by hand using a ceramic mortar and pestle to produce fine-grained powders for extraction) is not possible. Instead, we processed iron and fused silica samples for this study using a cryogenic ball mill (CryoMill; Retsch GmbH). This ball mill uses liquid nitrogen to cool the grinding jar, causing the iron meteorites to become brittle and able to be processed into powder and flakes; the cooler temperature also reduces the loss of volatile compounds. Samples were transferred into stainless steel grinding jars (50 mL) with stainless steel grinding balls (25 mm) that had been baked at 400 °C in air overnight. The 400 °C heating was employed to minimize the weakening of the steel jars and balls to mechanical stress. The samples were then ground using a program alternating four cooling cycles (5 Hz, 3 min) and four grinding cycles (30 Hz, 3 min); the alternating cycles ensured that heat created during grinding did not raise the temperature of the sample for a sustained period of time, but the exact temperature reached by the sample during each grinding cycle is unknown. Grinding jars were allowed to warm before opening to minimize condensation. The Imilac pallasite was first manually disaggregated using a ceramic mortar and pestle to separate metal and silicate fractions; the metal was then processed in the ball mill while the silicate was powdered using a ceramic mortar and pestle. It is worth noting that the CryoMilling process was not infallible; the grinding jars are designed to be used with larger volumes of softer material, and repeated use led to failure and breakage resulting in sample loss in two instances. These lost samples were not recovered for analyses due to contamination concerns. Figure S1 in supporting information shows representative iron meteorite samples before and after CryoMill processing.

After processing, portions (0.3–0.5 g) of each sample were flame-sealed separately in 20 mm borosilicate test tubes with 2 mL of ultrapure water and extracted at 100 °C for 24 h. Larger extraction tubes than typically used for stony meteorites (e.g., Glavin

et al. 2006) were required to provide additional headspace, as gas formation from metal–water reactions during the hot water extraction step tended to rupture smaller tubes. Large samples were split into multiple extraction portions; for example, the 0.7739 g sample of Canyon Diablo for unhydrolyzed analysis was extracted in two smaller portions. The extracts of these portions were combined following hot water extraction.

Extracts for hydrolyzed analysis were subjected to acid-vapor hydrolysis (3 h at 150 °C in the presence of doubly distilled 6N HCl). Both hydrolyzed and unhydrolyzed extracts were desalted using prepacked columns filled with cation-exchange resin (AG50W-X8, 100–200 mesh, hydrogen form, BIO-RAD) and the amino acids recovered by elution with 2 M NH_4OH (prepared from ultrapure water and NH_3(g) [Airgas], in vacuo). The desalted extracts were then derivatized using *o*-phthaldialdehyde/*N*-acetyl-L-cysteine (OPA/NAC) and analyzed (see the Determination of Amino Acid Abundances section).

Fused silica that had been baked overnight in air at 500 °C was processed in the cryogenic ball mill, extracted, desalted, derivatized, and analyzed in parallel with the meteorite samples. The measurements from the fused silica extracts reflect laboratory and processing background signals, and were used for background subtraction of the meteorite samples. Procedural blanks consisting of ultrapure water carried through the desalting and derivatization procedures were also analyzed. Based on previous analyses of amino acid standards taken through the entire hot water extraction and desalting procedure, there is no evidence of significant decomposition, racemization, and/or thermal degradation of the amino acids (Glavin et al. 2010).

Terrestrial Iron Control Samples

Iron granules (1–2 mm; Alfa Aesar; 99.98% [metal basis]) were used as an additional set of control samples to better understand the potential effects of our sample processing on the observed amino acid content. Although commercial high purity iron is pure with respect to other metals, the potential contamination of nonmetals such as carbon and nitrogen is not reported. Thus, our experiments were designed to test for contamination from sample processing as well as the potential synthesis of amino acids during milling. Iron was used as a control because the three iron meteorites analyzed (Campo del Cielo, Canyon Diablo, and Cape York) are principally composed of iron, with <10% nickel and other minor or components (Buchwald [1975] and references therein).

The commercial iron granules were first sieved to ensure that only the 1–2 mm size fraction was used. A portion of the granules was then coated (doped) with D-isovaline to serve as an amino acid tracer through the experiments; D-isovaline was chosen as a compound that is unlikely to be present from terrestrial contamination. Doping was accomplished by adding 25 g of granules to 10 mL of 2 μM D-isovaline and drying the solution in a centrifugal vacuum evaporator. A portion of these granules was then baked under vacuum at 500 °C for 5 days, and a subsample of these baked granules was then processed in the Cryomill following the same protocol as the meteorite samples. Finally, the milled samples were sieved and size-separated. Four subsets of the doped samples were then analyzed as below (see the Determination of Amino Acid Abundances section), including (1) "unbaked, unmilled" granules, to measure amino acid background of the commercial granules that had been coated with D-isovaline; (2) "baked, unmilled" granules, to determine whether baking provided externally clean iron granules, as verified by monitoring D-isovaline abundances; (3) "baked, milled" granules size 1–2 mm to determine the effects of milling on amino acid content; and (4) "baked, milled" granules <1 mm to determine effects of milling and granule size on amino acid content.

These samples were hot water extracted by refluxing ~3 g of each sample with 10 mL ultrapure water for 24 h in a 25 mL round bottom flask; this method was used instead of flame-sealing in test tubes to allow evolved H_2 to escape from the larger mass of iron being extracted. After extraction, samples were desalted using cation-exchange chromatography as described in the Meteorite Processing and Extraction section.

Determination of Amino Acid Abundances

Each desalted extract was analyzed for total amino acid content by ultrahigh-performance liquid chromatography with fluorescence detection and time-of-flight mass spectrometry (LC-FD/ToF-MS) using a Waters ACQUITY UPLC and Waters Xevo G2-XS Q-ToF-MS operating in positive electrospray ion mode. Because of the difficulty of extraction, the limited sample sizes, and the expected low abundances of amino acids, samples were concentrated prior to analysis; duplicate injections were made of the Campo del Cielo and Canyon Diablo measurements, while other meteorites had to be analyzed from a single injection.

Samples were first derivatized with OPA/NAC; specific details about the derivatization protocol and LC-FD/ToF-MS conditions used for amino acid analyses are given elsewhere (Glavin and Dworkin 2009; Glavin et al. 2021). In brief, derivatized samples were separated using tandem Waters BEH C18 column

(2.1 × 50 mm, 1.7 μm particle size)-Waters BEH phenyl column (2.1 × 150 mm, 1.7 μm particle size). Two different gradients were used. The first gradient is suitable for separation of most C_2 to C_6 aliphatic amino acids, while the second is optimized to separate the enantiomers and isomers of C_5 aliphatic amino acids. In both cases, the chromatographic conditions were: column temperature, 30 °C; flow rate, 150 μL min^{-1}; solvent A, 50 mM ammonium formate, 8% methanol, pH 8.0; solvent B, methanol. The C_2 to C_6 gradient was time in minutes (%B): 0 (0), 35 (55), 45 (100). The C_5-optimized gradient was time in minutes (%B): 0 (15), 25 (20), 25.06 (35), 44.5 (40), 45 (100). As in related studies, amino acids were identified by comparison with known standards using the masses and fluorescence responses of the OPA/NAC amino acid derivatives. Quantitation was performed using the single-ion mass traces to avoid the effects of interfering fluorescent peaks. Unless otherwise specified, chemicals and reagents were purchased from Sigma-Aldrich. A stock amino acid solution (1×10^{-6} M) was prepared by mixing individual amino acid standards (97–99% purity) in ultrapure water. The sources of the C_5 amino acid standards used are detailed elsewhere (Glavin and Dworkin 2009).

RESULTS

Amino Acids in Meteorite Samples

Amino acids were detected in all iron and pallasite meteorite samples at abundances above background levels, with total blank-subtracted concentrations ranging from 301 to 1216 pmol g^{-1} in the unhydrolyzed samples (Table 2). Acid hydrolysis of the iron meteorite hot water extracts produced results suggestive of amino acid destruction potentially caused by metal or cation abundances; therefore, all following results and discussion reference the unhydrolyzed data only. Tables 2 and 3 present the amino acid abundances in the extracts from the meteorite samples; Fig. S2 in supporting information shows the structures for the C_2–C_5 amino acids. Figure 1 shows a representative liquid chromatography-mass spectrum chromatogram of the unhydrolyzed extract from the Campo del Cielo meteorite, the fused silica control sample, and the standards. Terrestrial iron samples and other controls are discussed separately below.

The two-to-four carbon (C_2–C_4) amino acids detected in abundances ≥0.9 pmol g^{-1} in all unhydrolyzed samples include glycine, D- and L-alanine, β-alanine, D- and L- β-amino-*n*-butyric acid, γ-amino-*n*-butyric acid (γ-aba), and α-amino-isobutyric acid (α-AIB). A series of five-carbon (C_5) amino acids rare in biology was also observed in the iron meteorites; in particular, 3-aminopentanoic acid (3-apa), 4-aminopentanoic acid (4-apa), and 5-aminopentanoic acid (5-apa) were detectable in abundances ≥0.9 pmol g^{-1} in all iron meteorite samples; the silicate portion of the Imilac meteorite contained only trace amounts of 3-apa and 4-apa. Other C_5 amino acids were also observed (Table 3); however, these amino acids were present in trace abundances that were above the detection limit (0.1 pmol g^{-1}), but less than or close to the quantitation limit (0.9 pmol g^{-1}), of the analytical technique. Detection of the compounds is verified, but there are uncertainties in absolute quantitation, although it is possible to compare relative abundances of compounds. An attempt to extract larger sample amounts to increase compound abundances for analysis led to difficulties with increased interferences from mineral backgrounds and from the required desalting processing and was unsuccessful in increasing analyte signal.

Amino acids were detected in the hot water extracts of both the metal and silicate portions of the Imilac pallasite. The abundances in the silicate portion were much higher (1216 pmol g^{-1}) than in the iron portion (301 pmol g^{-1}), although a similar diversity of compounds was detected in both portions.

Tables 2 and 3 show that there is an L-excess of certain proteinogenic amino acids (aspartic acid, glutamic acid, serine, alanine, leucine, valine) in most of the meteorite samples. The nonproteinogenic amino acid β-amino-*n*-butyric acid is typically present in a racemic mixture or with a slight D-excess that is likely within the error of the measurements. Isovaline was not present in sufficient abundances to accurately measure the D/L ratio for most of the samples; D-isovaline was below the quantitation limit in all samples, and L-isovaline was quantifiable only in the Canyon Diablo sample.

Amino Acid Abundances in Control Samples

Multiple control and procedural blank samples were analyzed to understand potential background or contamination effects. Fused silica that had been baked overnight in air at 500 °C was processed in the cryogenic ball mill, extracted, desalted, derivatized, and analyzed in parallel with the meteorite samples. The fused silica extracts were used for background subtraction of the meteorite samples, as reflected in the data shown in Tables 2 and 3. Most amino acids were either not detected or present at very low abundances in the fused silica extracts, although higher levels of 5-apa and L-valine were observed (Fig. 1). The amino acids 5-apa and L-valine were also observed in procedural

Table 2. Summary of the abundances (pmol g^{-1}) of amino acids in the unhydrolyzed water extracts of the studied meteorites measured by LC-FD/Q-ToF-MS.[a]

Amino acids	Campo del Cielo[b]	Canyon Diablo[b]	Cape York[c]	Imilac metal[c]	Imilac silicate[c]
Dicarboxylic amino acids					
D-aspartic acid	tr	tr	1.9	1.3	6.2
L-aspartic acid	nd	3.5 ± 0.3	4.5	tr	44.6
D-glutamic acid	nd	nd	tr	tr	1.6
L-glutamic acid	nd	5.2 ± 1.0	1.3	nd	15.6
Hydroxy amino acids					
D-serine	tr	1.7 ± 0.1	1.5	2.0	14.6
L-serine	nd	38.7 ± 3.5	7.8	3.5	104.4
C_2 amino acid					
Glycine	364.7 ± 97.3	527.4 ± 64.4	272.8	190.2	802.4
C_3 amino acids					
β-alanine	37.4 ± 20.6	56.5 ± 8.3	42.8	53.7	82.1
D-alanine	9.0 ± 5.0	20.8 ± 2.2	7.8	6.9	16.4
L-alanine	18.5 ± 15.0	123.8 ± 17.1	15.0	10.7	57.3
C_4 amino acids					
DL-α-amino-*n*-butyric acid	3.0 ± 0.3	2.3 ± 0.3	1.6	1.8	tr
D-β-amino-*n*-butyric acid	2.9 ± 0.3	4.8 ± 0.3	2.7	1.2	5.1
L-β-amino-*n*-butyric acid	2.9 ± 0.2	4.7 ± 0.2	2.7	1.2	5.2
α-aminoisobutyric acid	3.4 ± 0.4	54.8 ± 0.4	5.0	2.0	8.9
γ-amino-*n*-butyric acid + β-aminoisobutyric acid	9.2 ± 0.4	17.7 ± 0.9	15.9	15.5	13.5
C_5 amino acids					
Total C_5 amino acids (Table 3)	17.4 ± 1.6	48.1 ± 2.7	6.9	7.6	8.9
C_6 amino acids					
ε-amino-*n*-caproic acid	nd	tr	2.8	tr	5.0
D-isoleucine	nd	nd	tr	tr	tr
L-isoleucine	tr	13.1 ± 0.1	1.4	1.8	14.9
D-leucine	tr	nd	tr	tr	tr
L-leucine	tr	8.1 ± 0.1	0.9	1.6	9.6
Total	468.4 ± 141.1	931.2 ± 99.2	395.3	301	1216.3

tr = detectable but below limit of quantitation (<0.9 pmol g^{-1}); nd = not detectable above procedural blank levels (<0.1 pmol g^{-1}).

[a]Extracts were analyzed by OPA/NAC derivatization and LC-FD/Q-ToF-MS. For the LC-FD/Q-ToF-MS data, the mono-isotopic masses of each protonated OPA/NAC amino acid derivative ($M + H^+$) were used for quantification and final peak integrations included background level correction using a procedural blank and a comparison of the peak areas with those of an amino acid standard run on the same day.

[b]Average of two measurements; standard deviation given.

[c]Single measurement only.

desalting blanks, suggesting a laboratory source for a portion of these compounds.

The exterior washes from the Campo del Cielo and Canyon Diablo meteorites were desalted, derivatized, and analyzed to examine potential contamination from the cutting and handling process. Analyses of the wash water from the Campo del Cielo sample showed increased levels (2–10 times greater) of L-enantiomers of the proteinogenic amino acids aspartic acid, glutamic acid, serine, and alanine compared to the analyses of the hot water extracts of the bulk meteorite sample. The Canyon Diablo wash did not show such large increases of the proteinogenic amino acids. In both wash samples, nonproteinogenic amino acids (β-alanine, β-amino-*n*-butyric acid, γ-aba, 5-apa, and 3-apa) were observed at levels lower than those detected in the hot water extracts of the bulk meteorite samples. Comparison of the wash water with the meteorite analyses showed that much of this contamination was removed by the washing process. For the C_5 amino acids, only 5-apa was detected in the wash water for both meteorites, while the wash for the Campo del Cielo meteorite contained low levels of 3-apa as well.

Terrestrial iron granules were also carried through the milling, extraction, desalting, derivatization, and analysis process (see the Terrestrial Iron Control Sample section). Table 4 summarizes results from these analyses; only the C_5 analytical gradient was used, leading to decreased ability to quantify or separate certain compounds. The unbaked, unmilled, "doped" sample showed the presence of low levels (0.1–0.5 ppb) of AIB, L- and D-alanine, and L-isovaline, as well as significant (>20 ppb) levels of glycine and the D-isovaline used as a dopant, and trace

Table 3. Summary of the abundances (pmol g^{-1}) of C_5 amino acids in the unhydrolyzed water extracts of the studied meteorites measured by LC-FD/Q-ToF-MS.[a]

C_5 amino acids	Campo del Cielo[b]	Canyon Diablo[b]	Cape York[c]	Imilac metal[c]	Imilac silicate[c]
D-norvaline (D-2-amino-*n*-pentanoic acid)	2.5 ± 0.2	tr	tr	tr	tr
L-norvaline (L-2-amino-*n*-pentanoic acid)	2.6 ± 0.2	tr	tr	tr	tr
D-isovaline (D-2-amino-2-methyl butyric acid)	nd	nd	nd	nd	nd
L-isovaline (L-2-amino-2-methyl butyric acid)	tr	tr	nd	nd	nd
D-valine (D-2-amino-3-methyl butyric acid)	tr	tr	nd	nd	nd
L-valine (L-2-amino-3-methyl butyric acid)	tr	16.1 ± 0.1	tr	tr	5.2
DL-3-amino-*n*-pentanoic acid (3-apa)	7.6 ± 0.1	4.6 ± 0.2	1.4	0.9	0.9
DL- and *allo*-3-amino-2-methyl butyric acid	tr	tr	tr	nd	nd
3-amino-3-methyl butyric acid	tr	tr	tr	tr	tr
3-amino-2,2-dimethyl propanoic acid	nd	nd	tr	nd	tr
DL-3-amino-2-ethyl propanoic acid	0.9	tr	tr	tr	tr
DL-4-amino-*n*-pentanoic acid (4-apa)	2.1 ± 0.2	2.8 ± 0.2	2.0	2.5	tr
DL-4-amino-2-methyl butyric acid	tr	tr	tr	tr	nd
DL-4-amino-3-methyl butyric acid	tr	tr	nd	nd	nd
5-amino-*n*-pentanoic acid (5-apa)	2.6 ± 0.9	24.6 ± 2.2	3.5	4.2	2.8
Total	17.4 ± 1.6	48.1 ± 2.7	6.9	7.6	8.9

tr = detectable but below limit of quantitation (<0.9 pmol g^{-1}); nd = not detectable above procedural blank levels (<0.1 pmol g^{-1}).

[a]Extracts were analyzed by OPA/NAC derivatization and LC-FD/Q-ToF-MS. For the LC-FD/Q-ToF-MS data, the mono-isotopic masses of each protonated OPA/NAC amino acid derivative ($M + H^+$) were used for quantification and final peak integrations included background level correction using a procedural blank and a comparison of the peak areas with those of an amino acid standard run on the same day.

[b]Average of two measurements; standard deviation given.

[c]Single measurement only.

detections of multiple other amino acids. Baking reduced amounts of all of these compounds to undetectable levels, with the exception of trace detections of AIB and serine, providing a clean iron sample surface with which to test the milling process. After milling to access the interior of the iron, analysis of the baked, milled iron revealed trace abundances of multiple C_5 amino acids and some C_2-C_4 amino acids, as well as higher abundances of glycine, D- and L-serine, β-alanine, L- and D-alanine, γ-ABA, α-AIB, and L-valine. These compounds were more abundant in the smaller (<1 mm) fraction produced after milling than in the larger (1–2 mm) fraction. Abundances were typically at trace levels below the quantitation limit. The relative abundance distributions were not the same as those observed in the iron meteorites, although the C_5 compounds present at highest abundances in the iron meteorites were also observed in the terrestrial iron. Figure S3 in supporting information shows chromatograms from the unbaked, milled, <1 mm fraction, as well as from a procedural blank and standard.

DISCUSSION

Amino Acid Abundances in Meteorite Samples and Sources

The presence of amino acids at low but detectable abundances in all iron and pallasite meteorite samples analyzed in this work is a new finding that requires care in interpreting and deciphering the source of the compounds. Some terrestrial contamination seems apparent on the surface of the samples, as indicated by the amino acid content observed in the water washes of the meteorite pieces, which contained excesses of proteinogenic amino acids (see the Amino Acid Abundances in Control Samples section). There is also some evidence of contamination in the milled meteorite samples, as shown by a marked excess of the L-enantiomers of protein amino acids, which suggests that some of the measured proteinogenic α-amino acids are due to terrestrial contributions; this likely includes portions of glycine, alanine, serine, glutamic acid, and aspartic acid for example. However, there is also evidence of indigenous amino acids within the milled meteorite samples. The amino acid abundances detected from the milled interior of the washed meteorites is distinctly different from the exterior washes, suggesting that these compounds are not simply present as surface contaminants. In addition, the presence of amino acids not commonly found in the terrestrial biosphere, such as the racemic β-amino-*n*-butyric acid, α-AIB, and the unusual suite of C_5 amino acids, suggests an indigenous component to the measured meteoritic amino acids, even though some of these compounds are present at very low abundances. Although stable isotopic ratios would also be a potential means of determining whether

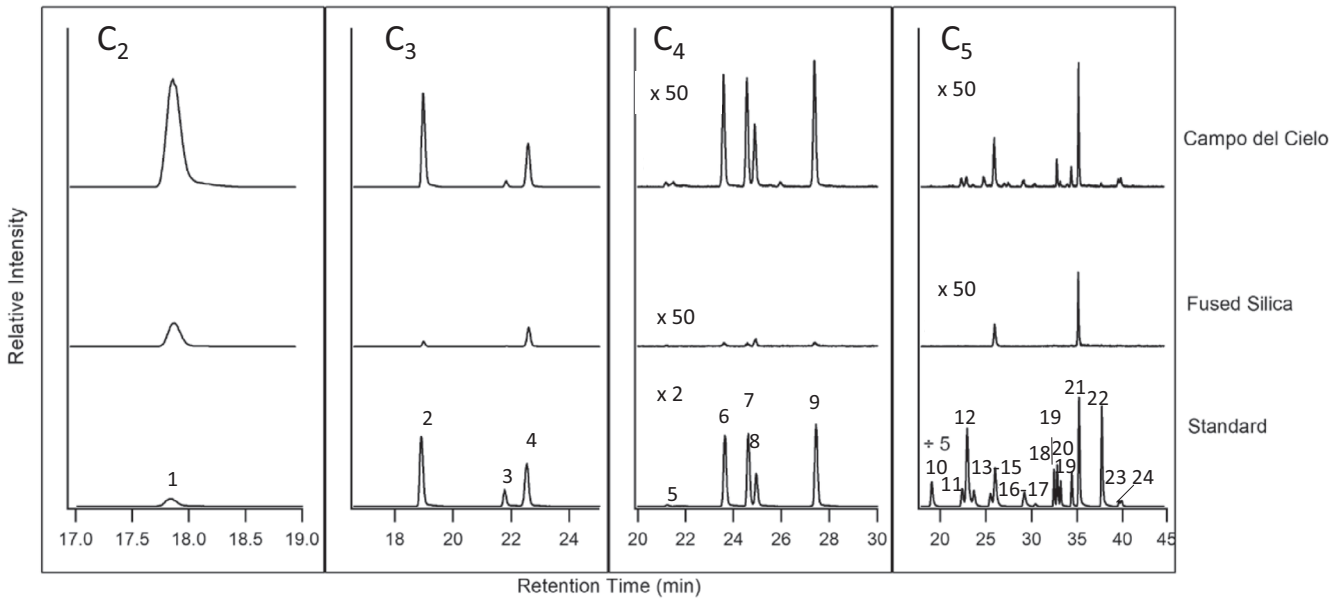

Fig. 1. Representative liquid chromatography-mass spectrometry chromatograms for the unhydrolyzed hot water extract of the Campo del Cielo meteorite and fused silica blanks compared to amino acid standards. Chromatograms shown are for the C_2, C_3, C_4, and C_5 primary, aliphatic, acyclic acids (derivatized positive ionization mass-to-charge ratios of 337.09, 351.10, 365.12, and 379.13, respectively). Traces are set to the same scale; in the C_4 and C_5 traces, peaks have been amplified by the factors given above each trace. See Fig. S2 for amino acid structures. Peaks were identified by comparison of the retention time and molecular mass to those in amino acid standards run on the same day and are designated by peak number as follows (1) glycine; (2) β-alanine; (3) D-alanine; (4) L-alanine; (5) γ-amino-*n*-butyric acid + D,L-β-aminoisobutyric acid; (6) D-β-amino-*n*-butyric acid; (7) L-β-amino-*n*-butyric acid; (8) α-aminoisobutyric acid; (9) D,L-α-amino-*n*-butyric acid; (10) 3-amino-2,2-dimethylpropanoic acid; (11) D,L-4-aminopentanoic acid; (12) D,L-4-amino-3-methylbutanoic acid; (13) D,L- and *allo*-3-amino-2-methylbutanoic acid; (14) D,L-3-amino-2-ethylpropanoic acid; (15) 5-aminopentanoic acid; (16) D,L-4-amino-2-methylbutanoic acid; (17) 3-amino-3-methylbutanoic acid; (18) D-isovaline; (19) D,L-3-aminopentanoic acid; (20) L-isovaline; (21) L-valine; (22) D-valine; (23) D-norvaline; (24) L-norvaline. The data used for this figure can be found in the supporting information.

the amino acids are due to terrestrial biological contamination, these measurements were not possible given the low abundances present and the difficulties associated with processing the large sample sizes that would be required for such measurements.

The contamination or terrestrial contribution to the amino acid content does not appear to be caused by the cryogenic milling apparatus, as the milled fused silica controls do not show amino acid abundances or distributions comparable to those observed in the meteorite samples (Fig. 1). Any contamination is most likely attributed to years spent in terrestrial environments and curation.

The various iron and pallasite samples show qualitative similarities in the relative abundances of the amino acids present, with the same suite of amino acids being most abundant in most samples. Quantitative comparisons are difficult because of the potential terrestrial components. Glycine is the most abundant amino acid in all hot water extracts samples analyzed in this work, but it is not possible to rule out a terrestrial contribution to the measured amounts. Excluding potential terrestrial contaminants, there does not appear to be a significant difference in the abundances of free amino acids between the two IAB meteorites (Canyon Diablo and Campo del Cielo) and the IIIAB meteorite (Cape York). This suggests that, at least in this small sample, the expected presence of silicate inclusions in the nonmagmatic IAB meteorites does not have a noticeable effect on the formation or preservation of amino acids relative to the lack of such inclusions in the magmatic IIIAB meteorite; note, however, that our analysis was of bulk (>1 cm^3) meteorite material and the abundance of silicate or graphite/troilite inclusions in the IAB samples is unknown. However, within the Imilac pallasite, the silicate portion contains higher amino acid abundances than the metal portion. This observation may suggest that the silicate material was a more favorable environment for amino acid formation mechanisms or amino acid preservation, that it may be a reflection of the low abundances of silicate or graphite/troilite inclusions that could favor these types of reactions in the metal portions of the meteorites, or that it may speak to the different formation history of Imilac from the iron meteorites.

Table 4. Summary of the abundances (pmol g^{-1}) of amino acids in the unhydrolyzed hot water extracts of terrestrial iron control samples measured by LC-FD/Q-Tof-MS.[a]

Amino acids	Unbaked, unmilled[b]	Baked, unmilled[c]	Baked, milled, 1–2 mm[d]	Baked, milled, <1 mm[e]
Dicarboxylic amino acids				
D-aspartic acid	*	*	*	*
L-aspartic acid	*	*	*	*
D-glutamic acid	*	*	*	*
L-glutamic acid	*	*	*	*
Hydroxy amino acids				
D-serine	tr	tr	2.6	6.7
L-serine	nd	1.5	1.7	8.3
C_2 amino acid				
Glycine	718.0	nd	112.9	329.3
C_3 amino acids				
β-alanine	3.8	nd	tr	2.7
D-alanine	1.2	nd	2.2	6.5
L-alanine	1.1	nd	5.2	18.6
C_4 amino acids				
DL-α-amino-*n*-butyric acid	tr	nd	tr	tr
D-β-amino-*n*-butyric acid	tr	nd	tr	tr
L-β-amino-*n*-butyric acid	tr	nd	tr	tr
α-aminoisobutyric acid	10.0	tr	tr	3.4
γ-amino-*n*-butyric acid + β-aminoisobutyric acid	tr	nd	tr	1.3
C_5 amino acids				
D-norvaline (D-2-amino-*n*-pentanoic acid)	tr	nd	tr	tr
L-norvaline (L-2-amino-*n*-pentanoic acid)	tr	nd	tr	tr
D-isovaline (D-2-amino-2-methyl butyric acid)	188[b]	nd	tr	tr
L-isovaline (L-2-amino-2-methyl butyric acid)	3.9	nd	nd	tr
D-valine (D-2-amino-3-methyl butyric acid)	nd	nd	tr	tr
L-valine (L-2-amino-3-methyl butyric acid)	tr	nd	tr	3.2
DL-3-amino-*n*-pentanoic acid (3-apa)	nd	nd	tr	tr
DL- and *allo*-3-amino-2-methyl butyric acid	nd	nd	nd	nd
3-amino-3-methyl butyric acid	tr	tr	nd	tr
3-amino-2,2-dimethyl propanoic acid	tr	nd	nd	tr
DL-3-amino-2-ethyl propanoic acid	nd	nd	nd	nd
DL-4-amino-*n*-pentanoic acid (4-apa)	tr	nd	tr	tr
DL-4-amino-2-methyl butyric acid	nd	nd	nd	tr
DL-4-amino-3-methyl butyric acid	nd	nd	nd	nd
5-amino-*n*-pentanoic acid	nd	nd	nd	tr
C_6 amino acids				
ε-amino-*n*-caproic acid	nd	nd	nd	nd
D-isoleucine	nd	nd	tr	tr
L-isoleucine	nd	nd	nd	tr
DL-leucine[f]	nd	nd	tr	tr

tr = detectable but below limit of quantitation (<0.9 pmol g^{-1}); nd = not detectable above procedural blank levels (<0.1 pmol g^{-1}).

[a]Extracts were analyzed by OPA/NAC derivatization and LC-FD/Q-ToF-MS. For the LC-FD/Q-ToF-MS data, the mono-isotopic masses of each protonated OPA/NAC amino acid derivative ($M + H^+$) were used for quantification and final peak integrations included background level correction using a procedural blank and a comparison of the peak areas with those of an amino acid standard run on the same day. All analyses are single measurements.

[b]Commercial iron granules were coated with D-isovaline as a tracer, but not otherwise processed.

[c]D-isovaline-coated granules were baked at 500 °C under vacuum for 5 days.

[d]Baked granules were cryomilled and sieved to 1–2 mm size fraction.

[e]Baked granules were cryomilled and sieved to <1 mm size fraction.

[f]Enantiomers not separated under gradient used.

*Not separated or quantifiable under gradient used.

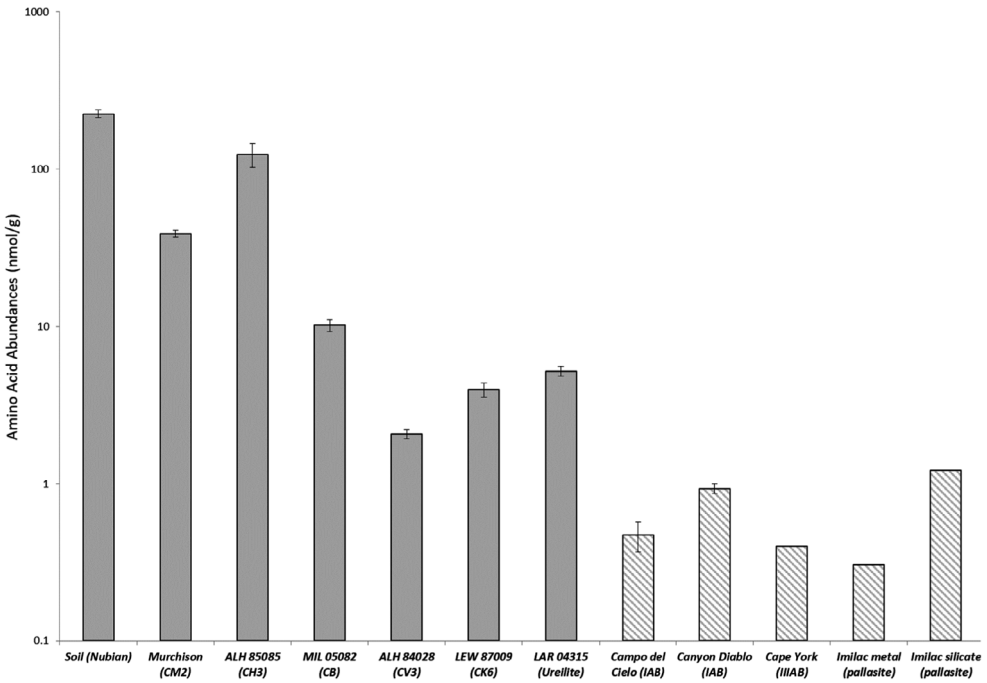

Fig. 2. A comparison of the amino acid abundances (nmol g^{-1}) in unhydrolyzed hot water extracts of the meteorites studied in this work (cross-hatched) with representatives of other meteorite types and terrestrial soil from the Nubian desert. Data sources: Soil (Burton et al. 2011); Murchison (Glavin et al. 2021); ALH 85085 and MIL 05082 (Burton et al. 2013); ALH 84028 and LAR 04315 (Burton et al. 2012); LEW 87009 (Burton et al. 2015). The data used for this figure can be found in the supporting information.

Figure 2 compares the amino acid abundances from unhydrolyzed hot water extracts of the meteorites in this study with representatives from other meteorite groups, including carbonaceous chondrites of different classes and alteration histories, as well as ureilites. The amino acid abundances in the iron and pallasite meteorites are much lower than those seen in carbonaceous chondrites, although the pallasite silicate portion is similar to the lowest abundances previously measured in two thermally altered CI-like chondrites (Burton et al. 2014b). This suggests that the formation/preservation conditions for amino acids in the metal meteorites (and in the metal portion of the pallasite) are not as favorable as those in the carbonaceous chondrites. Nonetheless, even these relatively low abundances could have made contributions to the early Earth or other primitive bodies.

The C_5 amino acids are less prone to terrestrial contamination, with more isomers that have not commonly been observed in terrestrial environments (e.g., Nubian soil analysis in Burton et al. [2011]; California soil analysis in Burton et al. [2014a]), and may provide more insight into the nature of the indigenous compounds. The most abundant C_5 amino acids in all iron samples were L-valine (a potential terrestrial contaminant), 3-apa, 4-apa, and 5-apa; 5-apa was also observed at lower levels in procedural blanks. Figure 3 shows distributions of the C_5 amino acids presented as a function of carbon structure and compared to data from terrestrial soil and carbonaceous chondrite meteorites. The observation that the straight chain amino acids (*n*-pentanoic acid variants; Fig. 3) were more abundant than the branched chain compounds (e.g., 4-amino-3-methylbutyric acid, also observed at trace levels in all iron meteorite samples) suggests that the formation mechanism leading to these compounds may favor straight chains over branched. It is also possible that some of these differences may be attributable to differences in thermal stability of amino acid isomers; for example, for C_4 amino acids, it has been shown that γ-aminobutyric acid is more stable to decarboxylation under aqueous conditions and elevated temperatures than α- and β-aminobutyric acid (Li and Brill 2003), and similar differences in stability may account for some of the C_5 distributions observed here.

The similarities in amino acid distributions (i.e., predominance of straight chain C_5 compounds) between all of the meteorites studied suggest a common formation mechanism or environment for the amino acids, not dependent on the chemical differences between these parent bodies. This type of straight chain dominance has been seen previously in thermally altered carbonaceous chondrites and ureilites (see Fig. 3, CV, CK, and ureilite

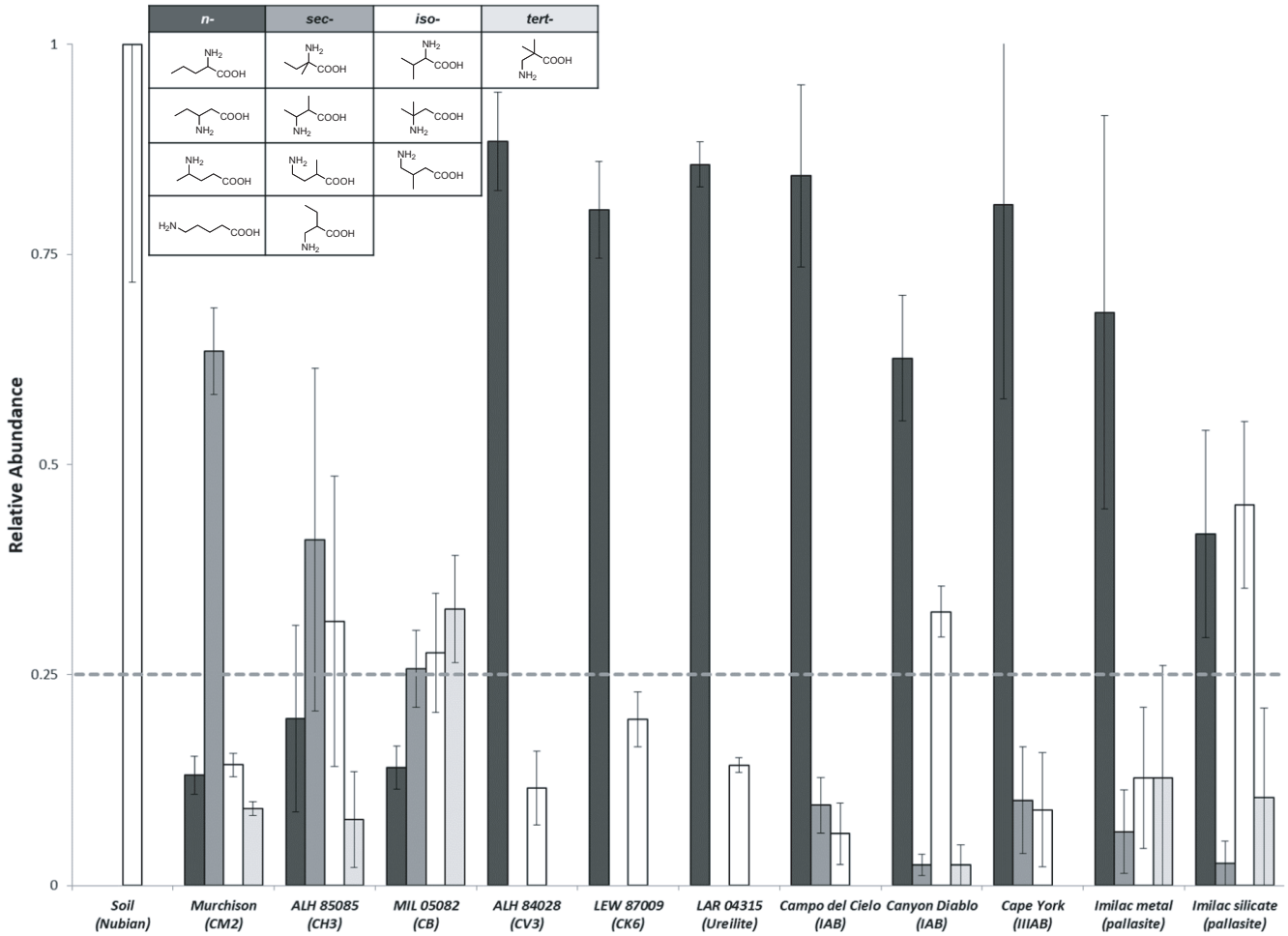

Fig. 3. A comparison of the relative abundances of the C_5 amino acids in unhydrolyzed hot water extracts of the iron and silicate meteorites studied in this work with representatives from other meteorite classes and terrestrial soil from the Nubian desert as a function of chain structure (*n*-, *sec*-, *iso*-, and *tert*-pentanoic acid) normalized to the total number of possible structural isomers. Inset shows the molecular structures and classifications of the C_5 isomers. The dashed line corresponds to the expected relative abundance if the amino acids were formed by a completely random synthetic process. See Fig. 2 caption for data sources. The data used for this figure can be found in the supporting information.

meteorites) and has been suggested to be a signature of surface-catalyzed formation mechanisms such as Fischer–Tropsch-type reactions (Burton et al. 2012). Fischer–Tropsch-type reactions occur between CO, H_2, and NH_3 on mineral grain surfaces; these reactions have been shown to produce amino acids and other organic compounds in laboratory studies and it has been debated that they could be responsible for meteoritic organic molecules (Hayatsu and Anders 1981; Cronin and Pizzarello 1990; Kerridge 1999). Given that the peak heating temperatures of the iron meteorite and pallasite parent bodies (>1300 °C for pallasites) would rapidly destroy amino acids, these types of reactions would have to occur during the cooling process, at temperatures <500 °C. Amino acids or other organics formed on the cooling parent body could then be preserved and delivered to the Earth's surface.

Figure 4 shows the relative abundances of the C_5 amino acids by amine position, again comparing the meteorites studied in this work with representative carbonaceous chondrites and ureilites. The iron meteorites contain relatively higher abundances of the δ-C_5 amino acid (5-apa) compared to other amine positions, although this is less prevalent in the Campo del Cielo meteorite. Again, these meteorites' relative abundances are most similar to the CV, CK, and ureilite meteorites studied previously, which suggests potential similarities in amino acid formation mechanisms.

One of the motivators for this work was the hypothesis, based on earlier observations of L-enantiomeric excesses of the C_5 amino acid isovaline in high-metal CH and CB carbonaceous chondrites, that interactions with metal surfaces could enhance

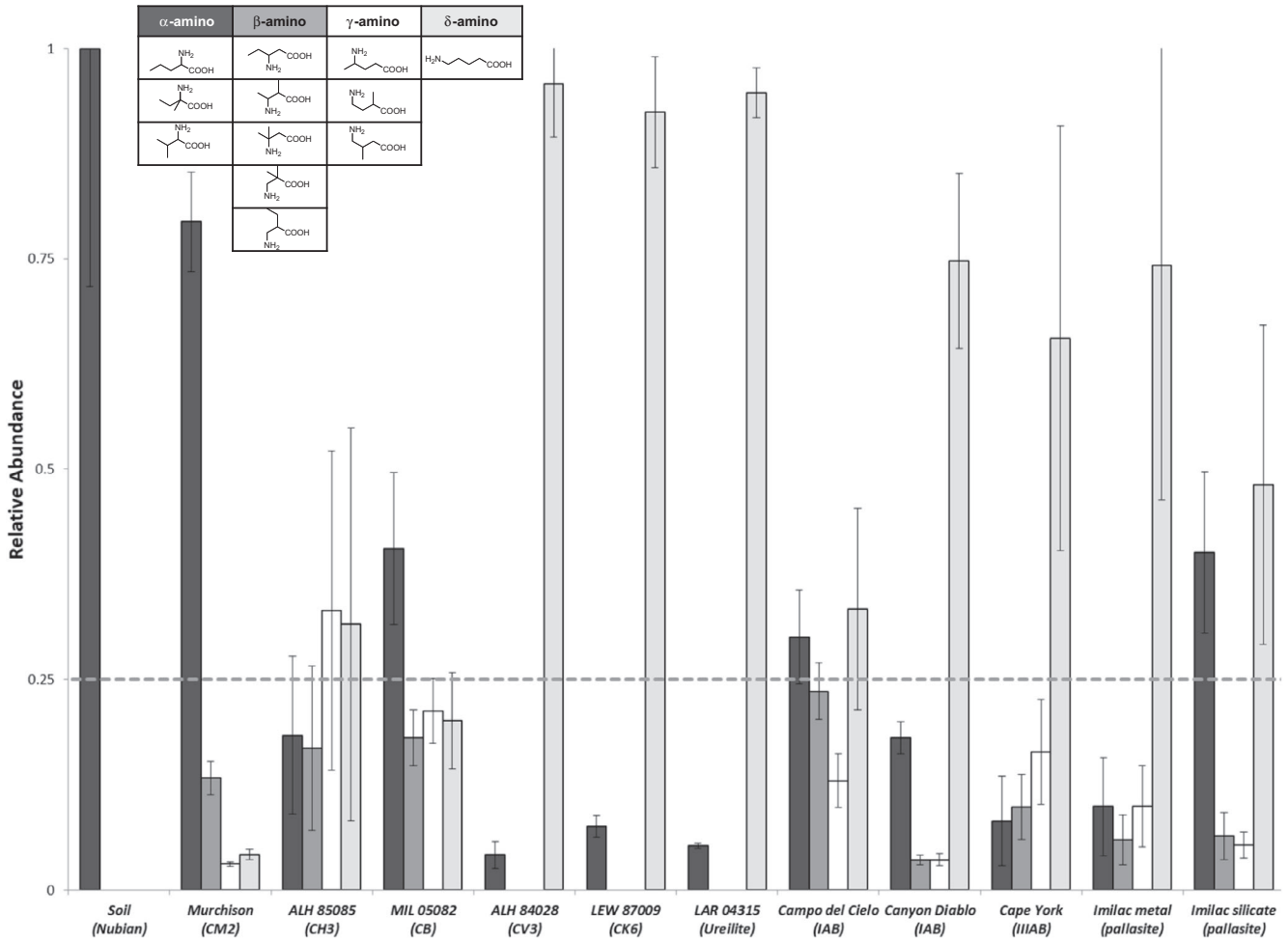

Fig. 4. A comparison of the relative abundances of the C_5 amino acids in unhydrolyzed hot water extracts of the iron and silicate meteorites studied in this work with representatives from other meteorite classes and terrestrial soil from the Nubian desert as a function of amine position (α-, β-, γ-, and δ-) normalized to the total number of possible structural isomers. Inset shows the molecular structures and classifications of the C_5 isomers. The dashed line corresponds to the expected relative abundance if the amino acids were formed by a completely random synthetic process. See Fig. 2 caption for data sources. The data used for this figure can be found in the supporting information.

enantiomeric excesses or chiral selection in meteoritic amino acids. Our observations did not support or refute this hypothesis, as low abundances meant that isomeric distributions could not be quantified in isovaline, and the only enantiomeric excesses observed were in proteinogenic amino acids and most likely caused by terrestrial contamination.

Amino Acids in Terrestrial Iron

The appearance of amino acids upon cryogenic milling of the terrestrial iron granules (Table 4) was surprising. It appears unlikely that these amino acids are surface contaminants transferred from laboratory materials during the processing and analysis, as fused silica carried through identical procedures did not contain these compounds (Fig. 1, middle trace). Milling into smaller grain sizes (<1 mm) produces 3–15× higher abundance of individual amino acids than milling without changing size (1–2 mm fraction). This observation suggests that amino acids are present in the iron, and that the additional milling exposes additional surface area for extraction. It is important to note that the 99.98% purity iron is on a metal basis, but we were unable to find any information on the carbon or nitrogen abundance in this or other commercial high purity iron (or nickel, their alloys, or other mineral proxies).

One potential explanation for the presence of these amino acids is that the reactions that led to the formation of the amino acids in the interior of the iron meteorites were also active in the environment in which

the terrestrial iron originated. The identity of these formation processes remains unknown, but catalytic reaction of amino acid precursors with metallic surfaces may be a possibility, as through Fischer–Tropsch/Haber–Bosch-type reactions.

A second possibility is that the milling process created amino acids from precursors that were present in both the meteorites and the terrestrial iron. A recent study showed that milling of precursors including aldehydes, ketones, amines, and potassium cyanide could drive the synthesis of α-aminonitriles in a one-pot Strecker reaction driven by mechanical processes (Hernández et al. 2016), while a second study indicated that milling iron cyano complexes can result in HCN, which can be trapped and incorporated into α-aminonitriles (Bolm et al. 2018). Such α-aminonitriles can convert to amino amides upon further milling (Bolm et al. 2018). These precursors could convert to amino acids upon extraction and hydrolysis. This mechanism, however, is only capable of producing the α-amino acids and would not be able to fully account for the other (non-α) amino acid isomers observed in our study, and hydrolysis was not performed in this study. However, it is possible that both the iron meteorite samples and terrestrial iron that we analyzed could have contained precursor molecules rather than free extractable amino acids that reacted during the milling process. Such grinding mechanical stress could have occurred on the early Earth, providing a mechanism for iron meteorites to deliver and release amino acids and their precursors. It is also possible that carbon inclusions, rather than precursor molecules, in the iron meteorite or the terrestrial iron reacted with N_2 during the milling process and/or with H_2 liberated during aqueous extraction to produce the observed compounds. Although we are not aware of reports of N_2 reactivity under these conditions, further work is required to test this hypothesis and determine its potential applicability to the early Earth.

CONCLUSIONS AND IMPLICATIONS

Our analyses show that iron meteorites can release low abundances of amino acids upon milling and hot water extraction and suggest that further study of the organic content of iron meteorites, as well as the potential origin of the amino acids observed within them, is needed. The distribution of amino acids differs from those observed in other meteorite classes, but is most similar to previous measurements from thermally altered meteorites, including CV and CK carbonaceous chondrites and ureilites. This distribution has previously been suggested to form via surface-catalyzed reactions of gases on metal surfaces, but it is not yet known if that mechanism could result in the distribution of compounds observed here. The observation of amino acids in the terrestrial iron granules subjected to milling suggests that similar processes may have occurred under terrestrial conditions.

The discovery of indigenous amino acids in iron meteorites adds to the potential sources of organic delivery to the early Earth. Since iron meteorites represent ~48% of meteoritic falls by mass (Grossman 2018; Korotev 2020), their contribution could have been significant. This finding, coupled with the potential for leaching of soluble organics through aqueous corrosion (Pasek and Lauretta 2005) and with recent studies of analog materials showing that hypervelocity impacts of iron meteorites on the early Earth could produce amino acids through coupling the reduction of atmospheric CO_2, atmospheric N_2, and H_2O with oxidation of metallic iron and nickel within the meteorites (Takeuchi et al. 2020), implies that the iron meteorites could have contributed to the early Earth's organic inventory in multiple ways.

Future studies of iron–nickel meteorites and asteroids may provide further insights into their potential organic inventory. NASA's Psyche mission will launch in 2022 and arrive at asteroid (16) Psyche in 2026, with the goal of mapping and studying this unique metal asteroid, which may be the exposed nickel–iron core of an early planet. The Psyche asteroid appears to be composed of 30–60% metal, with the remainder low-iron silicate rock; comparisons with meteorites suggest potential matches to pallasites or CB chondrites (Elkins-Tanton et al. 2020). The Psyche Gamma Ray and Neutron Spectrometer (GRNS) will perform elemental mapping of the asteroid; although carbon measurements are not a requirement for the instrument, based on previous similar analyses done at Mercury by the MESSENGER mission, it is reasonable to assume that if Psyche has carbon present at a few weight percent or higher, it is likely to be detected by the GRNS (Peplowski et al. 2015). Modeling efforts to characterize the gamma-ray signatures for carbon and other elements and signatures not considered during Psyche mission formulation are ongoing (Peplowski et al. 2018). Data from Psyche will lead to an understanding of the asteroid's formation and potential connections with meteorites in terrestrial collections and may help put the amino acid detections reported here in a larger context.

Acknowledgments—This work was funded by a grant from the Simons Foundation (SCOL award 302497 to JPD). We thank the Division of Meteorites, Department of Mineral Sciences, Smithsonian Institution for providing the meteorite samples for studies. We also

thank Dr. Tim McCoy and Dr. Nancy Chabot for helpful discussions and comments, and two anonymous reviewers for suggestions to improve this manuscript.

Data Availability Statement—The data that support the findings of this study are available in the supplementary material of this article.

Editorial Handling—Dr. Scott Sandford

REFERENCES

Bolm C., Mocci R., Schumacher C., Turberg M., Puccetti F., and Hernández J. G. 2018. Mechanochemical activation of iron cyano complexes: A prebiotic impact scenario for the synthesis of α-amino acid derivatives. *Angewandte Chemie International Edition* 57:2423–2426.

Buchwald V. F. 1975. *Handbook of iron meteorites. Their history, distribution, composition and structure*. Berkeley, California: University of California Press.

Burton A. S., Glavin D. P., Callahan M. P., Dworkin J. P., Jenniskens P., and Shaddad M. H. 2011. Heterogeneous distributions of amino acids provide evidence of multiple sources within the Almahata Sitta parent body, asteroid 2008 TC3. *Meteoritics & Planetary Science* 46:1703–1712.

Burton A. S., Elsila J. E., Callahan M. P., Martin M. G., Glavin D. P., Johnson N. M., and Dworkin J. P. 2012. A propensity for n-ω-amino acids in thermally altered Antarctic meteorites. *Meteoritics & Planetary Science* 47:374–386.

Burton A. S., Elsila J. E., Hein J. E., Glavin D. P., and Dworkin J. P. 2013. Extraterrestrial amino acids identified in metal-rich CH and CB carbonaceous chondrites from Antarctica. *Meteoritics & Planetary Science* 48:390–402.

Burton A. S., Glavin D. P., Elsila J. E., Dworkin J. P., Jenniskens P., and Yin Q. Z. 2014a. The amino acid composition of the Sutter's Mill CM2 carbonaceous chondrite. *Meteoritics & Planetary Science* 49:2074–2086.

Burton A. S., Grunsfeld S., Elsila J. E., Glavin D. P., and Dworkin J. P. 2014b. The effects of parent-body hydrothermal heating on amino acid abundances in CI-like chondrites. *Polar Science* 8:255–263.

Burton A. S., McLain H., Glavin D. P., Elsila J. E., Davidson J., Miller K. E., Andronikov A. V., Lauretta D., and Dworkin J. P. 2015. Amino acid analyses of R and CK chondrites. *Meteoritics & Planetary Science* 50:470–482.

Chabot N. L., Haack H., and McSween H. Y. 2006. Evolution of asteroidal cores. In *Meteorites and the early solar system II*, edited by Lauretta D. S. Tucson, Arizona: University of Arizona Press. pp. 747–771.

Cooper G., Jackson W. M., Rios A. C., Yeung K. J., and Dateo C. E. 2020. The origins of enantiomer excesses in meteoritic organic compounds: Were some reaction mechanisms directed by ambient magnetic and radiation fields? (abstract #3024). 51st Lunar and Planetary Science Conference. CD-ROM.

Cronin J. R. and Pizzarello S. 1990. Aliphatic hydrocarbons of the Murchison meteorite. *Geochimica et Cosmochimica Acta* 54:2859–2868.

Elkins-Tanton L. T., Asphaug E., Bell J. F. III, Bercovici H., Bills B., Binzel R., Bottke W. F., Dibb S., Lawrence D. J., Marchi S., McCoy T. J., Oran R., Park R. S., Peplowski P. N., Polanskey C. A., Prettyman T. H., Russell C. T., Schaefer L., Weiss B. P., Wieczorek M. A., Williams D. A., and Zuber M. T. 2020. Observations, meteorites, and models: A preflight Assessment of the composition and formation of (16) Psyche. *Journal of Geophysical Research: Planets* 125:e2019JE006296.

Elsila J. E., Aponte J. C., Blackmond D. G., Burton A. S., Dworkin J. P., and Glavin D. P. 2016. Meteoritic amino acids: Diversity in compositions reflects parent body histories. *ACS Central Science* 2:370–379.

Glavin D. P. and Dworkin J. P. 2009. Enrichment of the amino acid L-isovaline by aqueous alteration on CI and CM meteorite parent bodies. *Proceedings of the National Academy of Sciences* 106:5487–5492.

Glavin D. P., Dworkin J. P., Aubrey A., Botta O., Doty J. H. III, Martins Z., and Bada J. L. 2006. Amino acid analyses of Antarctic CM2 meteorites using liquid chromatography-time of flight-mass spectrometry. *Meteoritics & Planetary Science* 41:889–902.

Glavin D. P., Callahan M. P., Dworkin J. P., and Elsila J. E. 2010. The effects of parent body processes on amino acids in carbonaceous chondrites. *Meteoritics & Planetary Science* 45:1948–1972.

Glavin D. P., Alexander C. M. O. D., Aponte J. C., Dworkin J. P., Elsila J. E., and Yabuta H. 2018. The origin and evolution of organic matter in carbonaceous chondrites and links to their parent bodies. In *Primitive meteorites and asteroids*, edited by Abreu N. Amsterdam: Elsevier. pp. 205-271.

Glavin D. P., McLain H. L., Dworkin J. P., Parker E. T., Elsila J. E., Aponte J. C., Simkus D. N., Pozarycki C. I., Graham H. V., Nittler L. R., and Alexander C. M. O. D. 2020. Abundant extraterrestrial amino acids in the primitive CM carbonaceous chondrite Asuka 12236. *Meteoritics & Planetary Science* 55:1979–2006.

Glavin D. P., Elsila J. E., McLain H. L., Aponte J. C., Parker E. T., Dworkin J. P., Hill D. H., Connolly H. C. Jr, and Lauretta D. S. 2021. Extraterrestrial amino acids and L-enantiomeric excesses in the CM2 carbonaceous chondrites Aguas Zarcas and Murchison. *Meteoritics & Planetary Science* 56: 148–173.

Grady M. M. and Wright I. P. 2003. Elemental and isotopic abundances of carbon and nitrogen in meteorites. *Space Science Reviews* 106:231–248.

Grossman J. N. 2018. Meteorite Bulletin Database. https://www.lpi.usra.edu/meteor/metbull.php

Hayatsu R. and Anders E. 1981. Organic compounds in meteorites and their origins. In *Cosmo- and geochemistry*, edited by Bosche F. L. Berlin: Springer-Verlag. pp. 1–39.

Hayatsu R., Studier M. H., and Anders E. 1971. Origin of organic matter in early solar system—IV. Amino acids: Confirmation of catalytic synthesis by mass spectrometry. *Geochimica et Cosmochimica Acta* 35:939–951.

Hernández J. G., Turberg M., Schiffers I., and Bolm C. 2016. Mechanochemical strecker reaction: Access to α-aminonitriles and tetrahydroisoquinolines under ball-milling conditions. *Chemistry—A European Journal* 22:14513–14517.

Kerridge J. 1999. Formation and processing of organics in the early solar system. *Space Science Reviews* 90:275–288.

Korotev R. L. 2020. Some meteorite information. https://sites.wustl.edu/meteoritesite/items/some-meteorite-statistics/

Kruijer T. S., Burkhardt C., Budde G., and Kleine T. 2017. Age of Jupiter inferred from the distinct genetics and formation times of meteorites. *Proceedings of the National Academy of Sciences* 114:6712–6716.

Li J. and Brill T. B. 2003. Spectroscopy of hydrothermal reactions, part 26: Kinetics of decarboxylation of aliphatic amino acids and comparison with the rates of racemization. *International Journal of Chemical Kinetics* 35:602–610.

Nooner D. W. and Oró J. 1967. Organic compounds in meteorites. I. Aliphatic hydrocarbons. *Geochimica et Cosmochimica Acta* 31:1359–2000.

Pasek M. A. and Lauretta D. S. 2005. Aqueous corrosion of phosphide minerals from iron meteorites: A highly reactive source of prebiotic phosphorus on the surface of the early earth. *Astrobiology* 5:515–535.

Peplowski P. N., Lawrence D. J., Evans L. G., Klima R. L., Blewett D. T., Goldsten J. O., Murchie S. L., McCoy T. J., Nittler L. R., Solomon S. C., Starr R. D., and Weider S. Z. 2015. Constraints on the abundance of carbon in near-surface materials on Mercury: Results from the MESSENGER Gamma-Ray Spectrometer. *Planetary and Space Science* 108:98–107.

Peplowski P. N., Lawrence D. J., Beck A. W., Burks M., Chabot N. L., Goldsten J. O., Wilson J., Yokley Z. and Team P. M. S 2018. Nuclear spectroscopy of asteroid 16 Psyche (abstract #2114). 49th Lunar and Planetary Science Conference. CD-ROM.

Pizzarello S. 2012. Catalytic syntheses of amino acids and their significance for nebular and planetary chemistry. *Meteoritics & Planetary Science* 47:1291–1296.

Pizzarello S. and Groy T. L. 2011. Molecular asymmetry in extraterrestrial organic chemistry: An analytical perspective. *Geochimica et Cosmochimica Acta* 75:645–656.

Pizzarello S., Cooper G. W., and Flynn G. J. 2006. The nature and distribution of the organic material in carbonaceous chondrites and interplanetary dust particles. In *Meteorites and the early solar system II*, edited by Lauretta D. S. Tucson, Arizona: University of Arizona Press. pp. 625–651.

Rikken G. L. J. A. and Raupach E. 2000. Enantioselective magnetochiral photochemistry. *Nature* 405:932–935.

Rosenberg R. A. 2011. Spin-polarized electron induced asymmetric reactions in chiral molecules. In *Electronic and magnetic properties of chiral molecules and supramolecular architectures*, edited by Naaman R., Beratan D. N. and Waldeck D. Berlin: Springer. pp. 279–306.

Rosenberg R. A., Abu H. M., and Ryan P. J. 2008. Chiral-selective chemistry induced by spin-polarized secondary electrons from a magnetic substrate. *Physical Review Letters* 101:178301.

Sephton M. A. 2002. Organic compounds in carbonaceous meteorites. *Natural Products Reports* 19:292–311.

Sugiura N. 1998. Ion probe measurements of carbon and nitrogen in iron meteorites. *Meteoritics & Planetary Science* 33:393–409.

Takeuchi Y., Furukawa Y., Kobayashi T., Sekine T., Terada N., and Kakegawa T. 2020. Impact-induced amino acid formation on Hadean Earth and Noachian Mars. *Scientific Reports* 10:9220.

Yoshino D., Hayatsu R., and Anders E. 1971. Origin of organic matter in early solar system—III. Amino acids: Catalytic synthesis. *Geochimica et Cosmochimica Acta* 35:927–938.

SUPPORTING INFORMATION

Additional supporting information may be found in the online version of this article.

Fig. S1. Representative photographs of unprocessed (left) and CryoMill-processed (right) iron meteorite samples.

Fig. S2. Structures of C_2–C_5 amino acids analyzed in this study. Chiral centers are marked with an asterisk (*).

Fig. S3. Liquid chromatography-mass spectrometry chromatograms for the unhydrolyzed hot water extract of the baked, milled terrestrial iron (<1 mm fraction) and procedural blank compared to amino acid standards.

Data S1. Excel file containing all of the raw data used to generate the plots shown in Figs. 1–4.

SUPPORTING INFORMATION

Additional supporting information may be found in the online version of this article.

Data S1. Excel file containing all of the raw data used to generate the plots shown in Figs. 1-4.

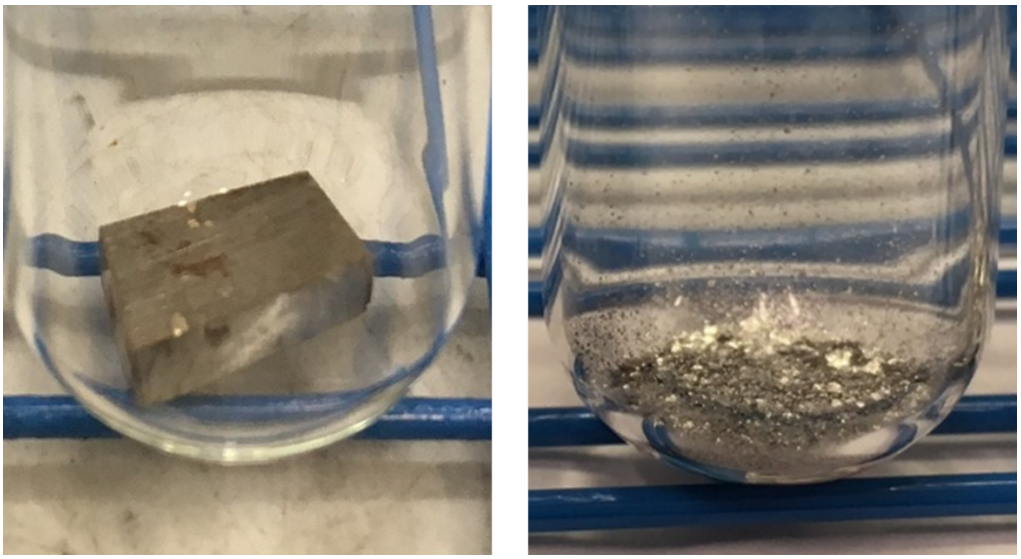

Figure S1. Representative photographs of unprocessed (left) and CryoMill-processed (right) iron meteorite samples. Samples are shown in 20-mm diameter test tubes.

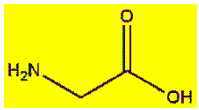

glycine

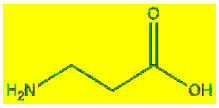

β-alanine

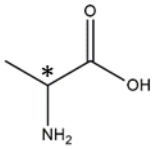

alanine

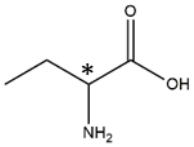

α-amino-*n*-butyric acid

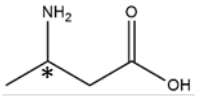

β- amino-*n*-butyric acid

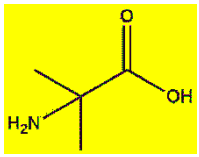

α- aminoisobutyric acid

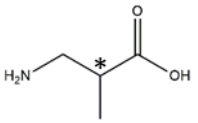

β-aminoisobutyric acid

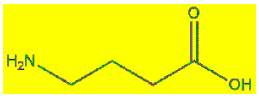

γ- amino-*n*-butyric acid

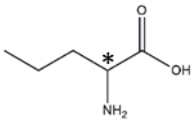

norvaline (2-amino-*n*-pentanoic acid)

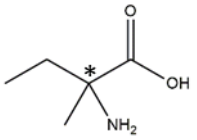

isovaline (2-amino-2-methyl butyric acid)

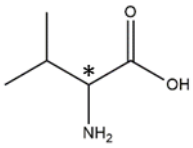

valine (2-amino-3-methyl butyric acid)

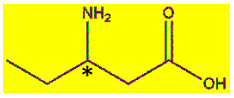

3-amino-*n*-pentanoic acid (3-apa)

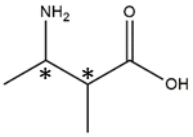

3-amino-2-methyl butyric acid

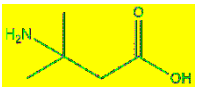

3-amino-3-methyl butyric acid

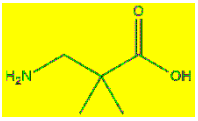

3-amino-2,2-dimethyl propanoic acid

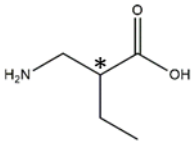

3-amino-2-ethyl propanoic acid

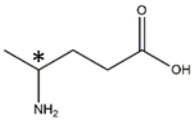

4-amino-*n*-pentanoic acid (4-apa)

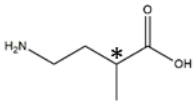

4-amino-2-methyl butyric acid

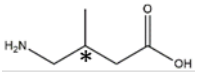

4-amino-3-methyl butyric acid

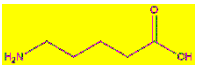

5-amino-*n*-pentanoic acid

Figure S2. Structures of C_2 to C_5 amino acids analyzed in this study. Chiral centers are marked with an asterisk (*).

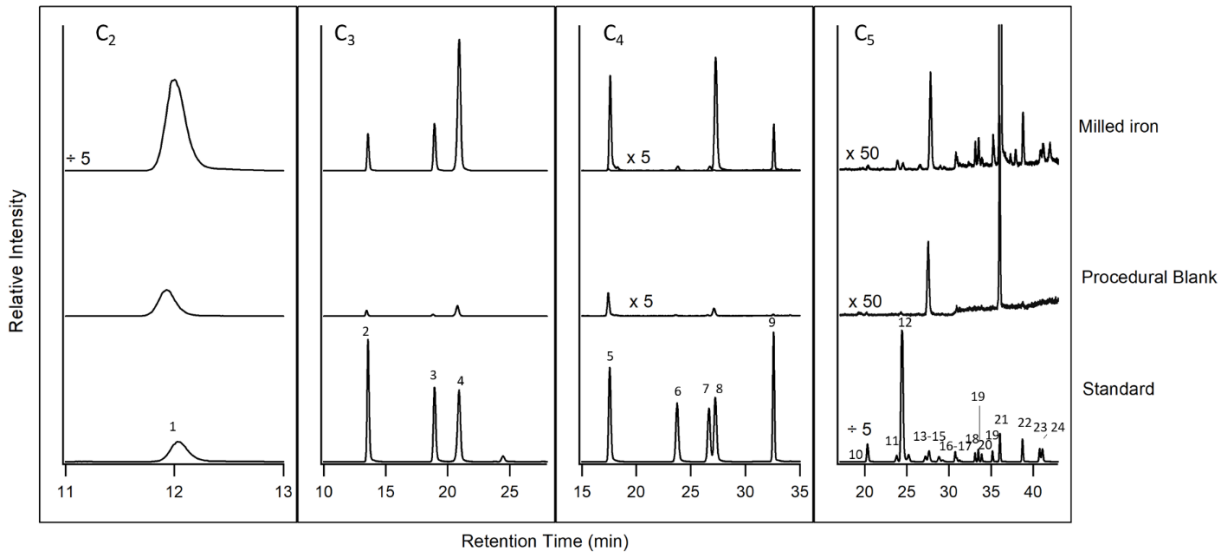

Figure S3. Liquid chromatography-mass spectrometry chromatograms for the unhydrolyzed hot-water extract of the baked, milled terrestrial iron (<1 mm fraction) and procedural blank compared to amino acid standards. Chromatograms shown are for the C_2, C_3, C_4, and C_5 primary, aliphatic, acyclic acids (derivatized positive ionization mass-to-charge ratios of 337.09, 351.10, 365.12, and 379.13, respectively). Traces are set to the same scale and are the same scale as Figure 1; peaks have been amplified by the factors given above each trace. See Figure S2 for amino acid structures. Peaks were identified by comparison of the retention time and molecular mass to those in amino acid standards run on the same day and are designated by peak number as follows: 1) glycine; 2) β-alanine; 3) D-alanine; 4) L-alanine; 5) ɣ-amino-*n*-butyric acid + D,L-β-aminoisobutyric acid; 6) D-β-amino-*n*-butyric acid; 7) L-β-amino-*n*-butyric acid; 8) α-aminoisobutyric acid; 9) D,L-α-amino-*n*-butyric acid; 10) 3-amino-2,2-dimethylpropanoic acid; 11) D,L-4-aminopentanoic acid; 12) D,L-4-amino-3-methylbutanoic acid; 13) D,L- and *allo*-3-amino-2-methylbutanoic acid; 14) D,L-3-amino-2-ethylpropanoic acid; 15) 5-aminopentanoic acid; 16) D,L-4-amino-2-methylbutanoic acid; 17) 3-amino-3-methylbutanoic acid; 18) D -isovaline; 19) D,L-3-aminopentanoic acid; 20) L-isovaline; 21) L-valine; 22) D -valine; 23) D -norvaline; 24) L-norvaline.